Impact of measurement dating inaccuracies in the monitoring of bulk material flows

Lionel MAGNIS, Nicolas PETIT

The Systems and Control Centre, MINES ParisTech, 60 Bd Saint-Michel, 75272 Paris Cedex, France

lionel.magnis@mines-paristech.fr, nicolas.petit@mines-paristech.fr

DOI: 10.15598/aeee.v13i1.1096

Abstract. *This paper discusses the negative impact of errors in the dating of information gathered across a distributed network of sensors to be treated by a centralized monitoring algorithm. In this contribution, an example of flow monitoring serves as basis for the analysis. We consider an estimator setup for loss detection. Using a simple probability model, we determine the variance of this estimator and show how it is impacted by the dating uncertainty. A mitigating solution is proposed. Further extensions are discussed.*

Keywords

Data synchronization, filtering, loss detection, network monitoring.

1. Introduction

In this article, we wish to stress the negative role on data analysis algorithms of dating inaccuracies of measurements. We base our discussion on a particular case of bulk material flow monitoring, but the reasoning could be generalized to other cases, and spur interest in this underestimated problem. To understand the issue under consideration here, let us now focus on flow monitoring applications. In various industrial fields, conveyor systems (or pipes) are used to transport bulk material from one inlet point to an outlet point, over possibly long distances, see [16]. These systems are subject to product losses (e.g due to hardware ageing) or thefts. Besides their obvious economical impact, these losses are caused for other numerous issues such as environmental disasters (e.g. oil leaks) or cascaded unreliability in downstream production processes (e.g. in a supply chain).

To prevent these malicious effects, numerous loss detection systems have been developed. A detection method commonly employed uses the law of conservation of mass to relate measurements from sensors distributed along the transport path. The resulting class of "balancing methods" evaluates the deviation in each part of the path between measured inlet and outlet mass or volume flow. In the oil industry, this method, also known as compensated mass balance (when the variation of density is accounted for, see [12]), is very popular. Its main advantages are the relative simplicity for actual implementation, the ease of tuning, the ability to uncover small leaks taking place over long time periods, along with its fast reaction to major leaks, see [6]. Considering the sensing technologies available for bulk material flow measurement (mostly laser or ultrasonic based, e.g. [9], [18]), this approach can be generalized to a wide class of bulk material conveyors.

Applying the conservation of mass principle based on information from spatially distributed sensors requires a good synchronization of data. The return of experience from several remarkable applications reported in the literature has served to formulate recommendations concerning the data acquisition technology, see [6]: *i)* the employed remote terminal units retrieving information from in-situ instruments should allow fast data transfer to the centralized master monitoring system, *ii)* the data should be carefully time-stamped with accurate and synchronized clocks (e.g. using GPS clock or Rugby clocks which, unfortunately, can be hardly available and subjected to jamming in many areas, or even SMS over cellular networks). Unfortunately, these recommendations are far from the technical status observed in currently installed systems. This is not surprising, as the problem of clock synchronization over a network is a complex one, even under the assumption of perfect two-way communications across the network, see [10], [11], and for this reason has been identified as a bottleneck in several control and monitoring architectures as described in [2], [13], [15], [19].

Let us now describe in more details the implementation of dating methodologies. As detailed in [1], the variation in reporting times from one data acquisition device (DAD) situated in one field location to the distant centralized supervisory control and data acquisition system (SCADA) can be quite large. The discussed time-stamping is usually not performed at the level of the DAD but the centralized SCADA level. The SCADA creates the time-stamp when the data is received. This procedure yields uncertainty on the age of data that are collected at the centralized level.

In this paper, we investigate the effect of time uncertainty on flow monitoring problem. Aiming at producing an analysis of the observations formulated by field practitioners, we conduct investigations on a "toy problem". As will appear, the model we propose shows that time uncertainty can produce false alarms in loss detection algorithms, which are usually considered as particularly annoying for production engineers. This underestimated problem can be as troublesome as the usual noises corrupting measurements. We believe that the conclusions that we draw here are sufficiently alarming to spur a general interest in this datation problem.

The paper is organized as follows. In Section 2. we formulate a simple transport model of a bulk material conveyor, the flow of which is monitored thanks to measurements produced by one inlet flow sensor and one outlet flow sensor. The measurements are produced almost periodically, due to the effect of a varying and unknown lag impacting each sample. Based on a probabilistic model of the lag value distribution, we establish the variance of the error introduced in the balance equation in Section 3. This balance relation serves as criterion for product-loss detection, and we relate the probability of detection and of false alarms to it. In Section 4. we determine flow pattern allowing one to minimize this variance. Simulations are presented in Section 5. stressing the role of data timing uncertainty, which, essentially increases the likelihood of false alarms.

2. Model and Problem Statement

Here, consider a bulk material conveyor with one input sensor DAD_I and one output sensor DAD_O as represented in Fig. 1. Each DAD gives a local measurement (q_I or q_O) of the material flow. Very generally, the sensors could be volume or mass flow meters (in the case of a pipeline as in the oil industry), or ultrasonic sensor (in the case of solid material, see [18], as in the mining or process industry [7]). The conveyor is assumed to generate a flow q having constant velocity v with respect to a fixed reference frame. Under this simplifying consideration, q is solution of a simple delay equation. This hypothesis is typically satisfied by conveyor belts used for solid materials. The situation is more complex for liquid pipelines, for which the water-hammer equation is usually considered, see [3] and [17], or for multiphase flow, see [8]. However, the approach advocated in this article can be extended, at the expense of including physics-based transformations, and possibly, reaction terms.

For this "toy problem", we wish to detect the occurrence of product losses by monitoring the sensor values. Note l the length between the two measurement locations. In accordance with the assumptions above, our simple model states that, in the absence of any product loss, q_I and q_O are related by the delay equation:

$$q_O\left(t+\frac{l}{v}\right) = q_I(t). \qquad (1)$$

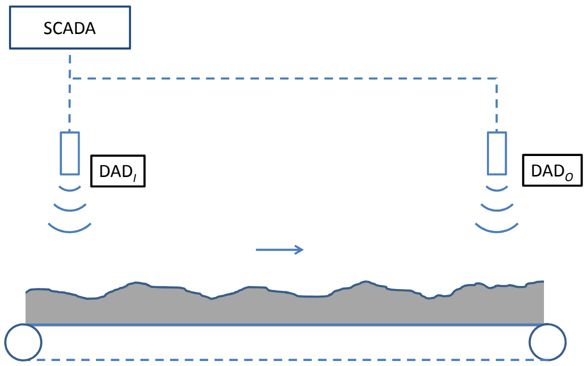

Fig. 1: Bulk material conveyor: two networked sensors communicate information to the SCADA.

For convenience, we assume that a loss has a linear effect on q_O, so that a fraction of the input flow is lost. The delay equation becomes:

$$q_O\left(t+\frac{l}{v}\right) = \lambda q_I(t), \qquad (2)$$

where λ is a parameter in $]0,1]$ representing the product loss. Considering that a loss can randomly appear along the transport path, λ is the realization of a random variable Λ with values in $]0,1]$, the occurrence of a loss being equivalent to the random event $\Lambda < 1$.

A simple way to detect the occurrence of losses is to monitor the mass imbalance over a time window of width T:

$$\int_0^T \left(q_I(t) - q_O\left(t+\frac{l}{v}\right)\right)\, dt, \qquad (3)$$

which equals 0 if $\lambda = 1$. Consistently with common practice and implementations, the input and output measurements are sampled at a frequency $\nu_s = \frac{T}{N}$, transmitted to and processed by the SCADA. Due to-ill synchronisation of sampling dates, buffering and various other sources of network processes, the sampling time at which the measurements q_O and q_I are processed by the SCADA may differ. Taking $T = 1$ (without loss of generality) and the clock of the DAD$_I$ as a reference, the inlet sensor provides N input measurements of the form:

$$y_I[i] = q_I\left(\frac{i+\frac{1}{2}}{N}\right) + n_i,\ i = 0, \ldots, N-1, \quad (4)$$

where n_i represents measurement noise. The synchronization discrepancies are modeled by a biased random time-shift (jitter) on the DAD$_O$ measurements.

Namely, the output measurements have the form:

$$y_O[i] = \lambda q_I\underbrace{\left(\frac{i+\frac{1}{2}}{N} + w_i\right)}_{\triangleq t_i} + n'_i,\ i = 0, \ldots, N-1, \quad (5)$$

where n'_i represents measurement noise, and w_i is the realization of a zero-mean random variable W_i and we have assumed that the delay $\frac{l}{v}$ and the known average communication lag have been compensated by the appropriate time-shift.

A typical loss detection algorithm compares a discrete version of Eq. (3) such as:

$$b \triangleq \frac{1}{N}\sum_{i=0}^{N-1}(y_I[i] - y_O[i]), \quad (6)$$

against a threshold value b^*, rising a loss flag when $b \geq b^*$.

In the following, we study in details the effects of the law of the time uncertainty random variables W_i on this detection algorithm.

3. Imbalance Estimator

3.1. Preliminary Assumptions

Consider the two following assumptions.

Assumption 1. *The W_i have support in $[-\delta, \delta]$ with $\delta < \frac{1}{2N}$. Thus, for any realization of the W_i, one has $0 < t_0 < \ldots t_{N-1} < 1$.*

Assumption 2. *q_I is continuous on $[0, 1]$ and affine on every $[\frac{i}{N}, \frac{i+1}{N}]$.*

The parameter δ scales the time uncertainty. Note a_i the slope of $\frac{q_I}{N}$ on $[\frac{i}{N}, \frac{i+1}{N}]$. We have, for all i,

$$y_O[i] = \lambda q_I\left(\frac{i+\frac{1}{2}}{N}\right) + N\lambda a_i w_i + n'_i. \quad (7)$$

Without loss of generality, the total amount of bulk material entering the conveyor over the time window between 0 and 1 is unitary, i.e.:

$$1 = \int_0^1 q_I(t)dt. \quad (8)$$

As q_I is affine on every $[\frac{i}{N}, \frac{i+1}{N}]$, we have, exactly,

$$1 = \frac{1}{N}\sum_{i=0}^{N-1} q_I\left(\frac{i+\frac{1}{2}}{N}\right), \quad (9)$$

and the imbalance estimator is:

$$b = 1 - \lambda - \lambda\sum_{i\in\mathcal{I}} a_i w_i + \frac{1}{N}\sum_{i=0}^{N-1}(n_i - n'_i), \quad (10)$$

where $\mathcal{I} = \{i = 0, \ldots, N-1 \mid a_i \neq 0\}$.

In the following, we assume that $\mathcal{I}$ is nonempty, so that the flow is not constant on the considered time-window.

3.2. Estimator Probability Law

To emphasize the effect of time uncertainty, we first consider a noise-free case where $n_i = n'_i = 0$. Then, b appears as the realization of the random variable:

$$B = 1 - \Lambda - \Lambda\sum_{i\in\mathcal{I}} a_i W_i. \quad (11)$$

To establish the probability law of B, we assume that:

- Λ and the W_i are jointly independent,
- the W_i are identically distributed (IID) and have a continuous probability density function (*pdf*) f^W (with support $[-\delta, \delta]$),
- to account for the likelihood of a no-loss scenario, Λ has a mixed-law comprising a Dirac at $\lambda = 1$ and a continuous density h on an interval $[\alpha, \beta] \subset]0, 1]$, so that the *pdf* of λ is of the form:

$$f^\Lambda(\lambda) = ph(\lambda) + (1-p)\delta_1(\lambda), \quad (12)$$

where $p = P(\Lambda < 1)$ is the probability of occurrence of a loss.

By the formula of total probability, the *pdf* f^B of B can be recovered as:

$$f^B(b) = pf_L(b) + (1-p)f_{\bar{L}}(b), \quad (13)$$

where f_L (respectively $f_{\bar{L}}$) is the *pdf* of B conditional to the loss event $\Lambda < 1$ (respectively the loss-free event $\Lambda = 1$). For $\lambda = 1$, we have $b = -\sum_{i\in\mathcal{I}} a_i w_i$. Hence,

$$f_{\bar{L}}(b) = \circledast_{i\in\mathcal{I}} \frac{1}{|a_i|} f^W\left(\frac{\cdot}{-a_i}\right)(b), \quad (14)$$

where $\circledast$ designates multiple convolution products. On the other hand, for any $\lambda \in [\alpha, \beta]$, $b = 1 - \lambda - \lambda \sum_{i \in \mathcal{I}} a_i w_i$. Hence,

$$f_L(b) = \int_\alpha^\beta \frac{1}{\lambda} f_{\bar{L}} \left(\frac{b - 1 + \lambda}{\lambda} \right) h(\lambda) d\lambda. \tag{15}$$

Example 1. *We take:*

$$N = 10, \; p = 0.5, \; a_i = \sin \left(\frac{i}{N} \right). \tag{16}$$

We assume that the W_i are independent Beta variables, see [14], of parameter $(2, 2)$ with support in $[-\delta, \delta]$, namely:

$$f^W(w) = \frac{3}{4\delta^3} (\delta^2 - w^2) \mathbb{1}_{[-\delta,\delta]}(w) \tag{17}$$

and that, h is uniform on $[\alpha, \beta] = [0.6, 0.9]$. In Fig. 2, we represent $f_{\bar{L}}$, f_L and eventually f^B for $\delta = 0.01$ and $\delta = 0.04$. The larger the time uncertainty δ, the more the two modes of the pdf of B overlap.

3.3. Conditional Probability of a Loss Given the Measurement b

Consider the accuracy of measurement ε. A measured value b guarantees that $B \in I_\varepsilon \triangleq]b - \varepsilon, b + \varepsilon[$. We note:

$$p_L(b) \triangleq P_{B \in I_\varepsilon}(\Lambda < 1), \tag{18}$$

the conditional probability of a loss given $B \in I_\varepsilon$.

As illustrated in Fig. 2, the supports of $f_{\bar{L}}$ and f_L depend on the value of δ (and of α, β and the a_i). Indeed, note:

$$|a|_1 = \sum_{i=0}^{N-1} |a_i|. \tag{19}$$

According to Eq. (14) and Eq. (15), the respective supports $S_{\bar{L}}$ and S_L of $f_{\bar{L}}$ and f_L are, assuming $\delta |a|_1 \le 1$:

$$S_{\bar{L}} = [-\delta |a|_1, \delta |a|_1], \tag{20}$$

$$S_L = [1 - \beta(1 + \delta |a|_1), 1 - \alpha(1 - \delta |a|_1)], \tag{21}$$

and we have:

$$p_L(b) = 1, \; \forall b \in S_L \setminus S_{\bar{L}}, \tag{22}$$

$$p_L(b) = 0, \; \forall b \in S_{\bar{L}} \setminus S_L. \tag{23}$$

Hence, if $S_L \cap S_{\bar{L}}$ is empty, the value of $p_L(b)$ is either 0 or 1 and the measure of b indicates a loss without any ambiguity. Both supports are disjoint if and only if:

$$\beta(1 + \delta |a|_1) < 1 - \delta |a|_1. \tag{24}$$

Condition Eq. (24) fails to be met when the time uncertainty becomes too large, namely when:

$$\delta \ge \frac{1 - \beta}{|a|_1 (1 + \beta)}. \tag{25}$$

This is illustrated in Fig. 2. In such a case, a measure of $b \in S_L \cap S_{\bar{L}}$ is ambiguous. The Bayes formula [14] yields:

$$\begin{aligned} p_L(b) &= \frac{p P_{\Lambda<1}(B \in I_\varepsilon)}{p P_{\Lambda<1}(B \in I_\varepsilon) p + (1-p) P_{\Lambda=1}(B \in I_\varepsilon)} \\ &= \frac{p \int_{I_\varepsilon} f_L(x) dx}{p \int_{I_\varepsilon} f_L(x) dx + (1-p) \int_{I_\varepsilon} f_{\bar{L}}(x) dx} \\ &= \frac{p f_L(b)}{p f_L(b) + (1-p) f_{\bar{L}}(b)} + O(\varepsilon^2). \end{aligned} \tag{26}$$

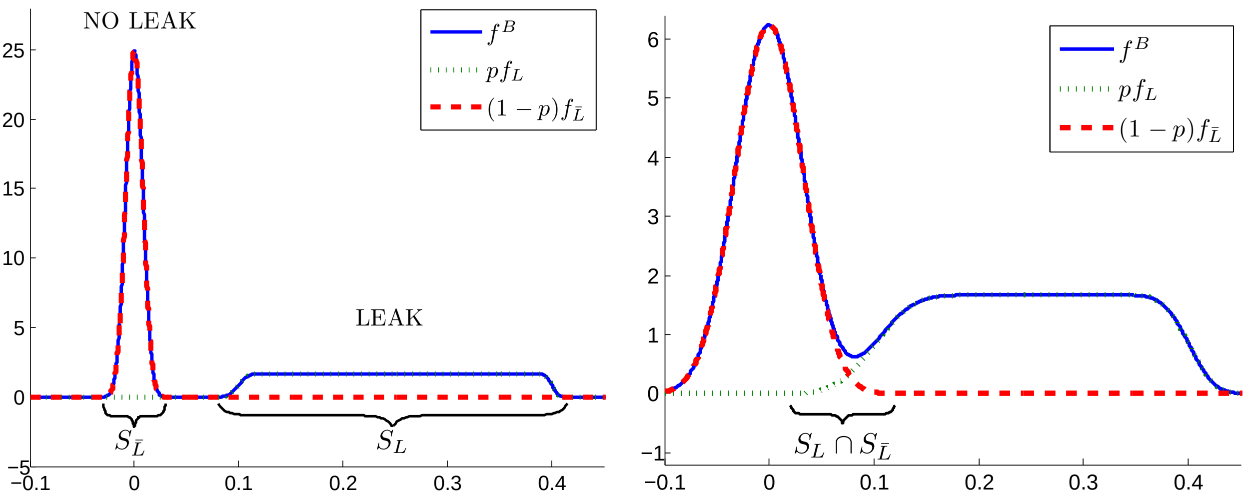

Fig. 2: *pdf* of B with parameters of Exm. 1 for $\delta = 0.01$ (left) and $\delta = 0.04$ (right). On the right, the overlap generated by the time uncertainty causes some ambiguity.

This probability is represented in Fig. 3 for the parameter values of Exm. 1 and various values of δ. The probability p_L varies from 0 to 1 with a slope, which gets steeper as δ decreases. In the extreme case $\delta = 0$, the probability is a step from 0 to 1, in which case the measurement b allows to identify a loss without ambiguity. The bigger δ, the further from this ideal case, the harder it is to identify a loss.

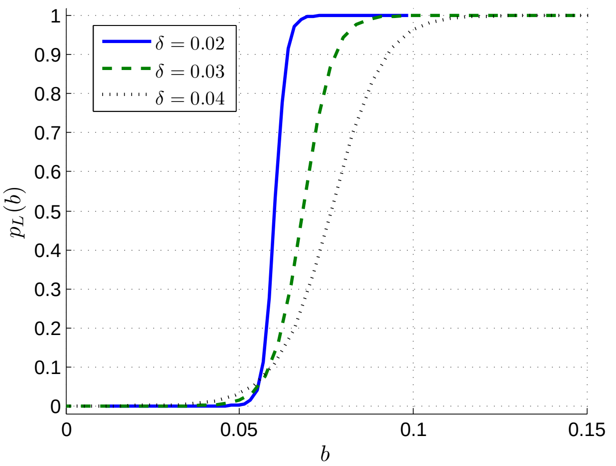

Fig. 3: Probability of a loss for values of b in the ambiguous zone.

3.4. Loss Detection and False Alarms

For a given threshold value b^*, we are interested in:

- the probability p_D of detecting a loss,
- the probability p_F of an alarm being false.

We have:

$$p_D = P_{\Lambda<1}(b \geq b^*) = \int_{b^*}^{\infty} f_L(b)db, \quad (27)$$

$$p_F = P_{b \geq b^*}(\Lambda = 1) = \frac{(1-p)\int_{b^*}^{\infty} f_{\bar{L}}(b)db}{\int_{b^*}^{\infty} f^B(b)db}. \quad (28)$$

Ideally, one wants p_D as close to 1 as possible to detect most losses, and p_F as low as possible to avoid false alarms. These probabilities decrease as the threshold grows. We represent p_D and p_F in Tab. 1 for various values of these parameters.

3.5. Impact of Measurement Noise

For realism, we now add measurement noise to the model and assume that, for all i, n_i (respectively n'_i) is the realization of a random variable N_i (respectively N'_i) and that the N_i (respectively N'_i) are IID zero-mean Gaussian variables with standard deviation σ_0 (respectively σ_1). We also assume that all the random variables of the problem are jointly independent. With these assumptions, Eq. (11) becomes:

$$B = 1 - \Lambda - \Lambda \sum_{i \in \mathcal{I}} a_i W_i + \frac{1}{N} \sum_{i=0}^{N-1} (N_i - N'_i), \quad (29)$$

where:

$$\frac{1}{N} \sum_{i=0}^{N-1} (N_i - N'_i) \quad (30)$$

is a zero-mean Gaussian variable with standard deviation:

$$\sqrt{\frac{\sigma_0^2 + \sigma_1^2}{N}}. \quad (31)$$

Hence, the *pdf* f^B computed in Section 3.2. is simply convolved with a Gaussian *pdf*, and the same applies to $f_{\bar{L}}$ and f_L. As a result, p_D and p_F are altered as is reported in Tab. 1, with $\sigma_0 = 0.1$ and $\sigma_1 = 0.05$.

To sum-up the information gathered in Tab. 1, we can conclude that:

- the tuning of b^* results from a trade-off between the detection capabilities and the desired reliability of the loss-detection algorithm. This tuning is however difficult, as p_D and p_F also depend on the time uncertainty scaled by δ,
- for any fixed threshold value b^*, the performance of the loss-detection algorithm deteriorates with δ.

Tab. 1: Performances of loss-detection algorithm deteriorate with time uncertainty δ, p_D (probability of loss detection), p_F (probability of false alarm).

Threshold, case without noise	$\delta = 0.02$		$\delta = 0.03$		$\delta = 0.04$	
	p_D	p_F	p_D	p_F	p_D	p_F
$b^* = 0.03$	1.000	0.024	1.000	0.086	1.000	0.137
$b^* = 0.07$	0.999	0.000	0.996	0.001	0.991	0.011
$b^* = 0.11$	0.951	0.000	0.944	0.000	0.936	0.000
Threshold, case with noise						
$b^* = 0.03$	0.999	0.167	0.998	0.180	0.996	0.194
$b^* = 0.07$	0.984	0.031	0.981	0.043	0.976	0.059
$b^* = 0.11$	0.927	0.002	0.922	0.004	0.917	0.009

4. Choice of an Optimal Input Flow Pattern

Time uncertainty has no effect under steady flow conditions, as the a_i are all zero and, irrespective of the time uncertainty, the measurements will be identical (up to noise). The detrimental effect of time uncertainty on the detection algorithm performance will appear for transient flow patterns. Then, a natural question is to determine a way to alleviate these effects. As will appear, an active control strategy brings a possible solution. In this section we assume that the conveyor has an actuator at the input point so that one can choose the input pattern q_I. The problem we consider is the scheduling of the flow for a sudden overload consisting of a unitary amount of bulk material spread over a unitary time. We investigate the choice of an "optimal" input pattern q_I with respect to loss detection.

Consider a fixed value for λ. The expectancy of B conditional to $\Lambda = \lambda$ is exactly the imbalance. Indeed, one has:

$$\begin{aligned} \mathbb{E}\left(1 - \lambda - \lambda \sum_{i\in\mathcal{I}} a_i W_i + \frac{1}{N}\sum_{i=0}^{N-1}(N_i - N_i')\right) \\ = 1 - \lambda. \end{aligned} \tag{32}$$

The variance of B conditional to $\Lambda = \lambda$ is in Eq. (44), where σ_W is the standard deviation of the IID W_i. Decreasing σ seems promising for loss-detection, as the bias estimator will all the more accurately represent the true imbalance $1 - \lambda$. We have, for all i,

$$\begin{aligned} q_I(t) = q_I(0) + N a_i\left(t - \frac{i}{N}\right) + \\ + \sum_{j=0}^{i-1} a_j, \forall t \in \left[\frac{i}{N}, \frac{i+1}{N}\right]. \end{aligned} \tag{33}$$

Starting from and returning to a steady flow q_n, we consider equations:

$$q_I(0) = q_I(1) = q_n, \quad \int_0^1 (q_I(t) - q_n)dt = 1, \tag{34}$$

which directly translate into two affine constraints bearing on the a_i:

$$\underbrace{\sum_{i=0}^{N-1} a_i = 0}_{\triangleq g_1(a)}, \quad \underbrace{N + \sum_{i=0}^{N-1} i a_i = 0}_{\triangleq g_2(a)}. \tag{35}$$

Thus, in view of Eq. (44), we consider the following problem.

Problem 1. *Find $a = (a_0, \ldots, a_{N-1})$ minimizing*

$$|a|_2 = \sqrt{\sum_i |a_i|^2} \tag{36}$$

under the affine constraints (35).

Solution 1. *Problem 1 has a unique solution $a^{\#}$ given by*

$$a_i^{\#} = \frac{6}{N+1} - \frac{12\ i}{N^2-1}, \quad \forall i = 0, \ldots, N-1. \tag{37}$$

Note $q^{\#}$ the corresponding flow. The associated variance is:

$$\sigma^2 = \frac{12N}{N^2-1}\lambda^2\sigma_W^2 + \frac{\sigma_0^2 + \sigma_1^2}{N}. \tag{38}$$

Proof 1. *As $|.|_2$ is convex and radially unbounded, it reaches a unique minimum under the affine constraints. Note $f(a) \triangleq \frac{|a|_2^2}{2}$. Then $a^{\#}$ satisfies the Lagrangian equation [4]:*

$$\begin{aligned} \nabla f(a) = \lambda_1 \nabla g_1(a) + \lambda_2 \nabla g_2(a) \\ \Leftrightarrow \ a_i = \lambda_1 + i\ \lambda_2, \ \forall i. \end{aligned} \tag{39}$$

Injecting these relations into the constraint $g_1(a) = 0$ yields:

$$N\lambda_1 + \lambda_2 \sum_{i=0}^{N-1} i = 0 \ \Leftrightarrow \ \lambda_1 = \frac{1-N}{2}\lambda_2. \tag{40}$$

Injecting:

$$a_i = \left(\frac{1-N}{2} + i\right)\lambda_2, \quad \forall i \tag{41}$$

into the constraint $g_2(a) = 0$ yields:

$$\begin{aligned} \lambda_2\left(\frac{1-N}{2}\sum_{i=0}^{N-1} i + \sum_{i=0}^{N-1} i^2\right) = -N \\ \Leftrightarrow \ \lambda_2 = \frac{-12}{N^2-1}. \end{aligned} \tag{42}$$

Hence, $a^{\#}$ satisfies, for all i:

$$\begin{aligned} a_i^{\#} &= \frac{-12}{N^2-1} \times \frac{1-N}{2} - \frac{12}{N^2-1}\ i \\ &= \frac{6}{N+1} - \frac{12\ i}{N^2-1}. \end{aligned} \tag{43}$$

Then calculation of the variance is straightforward.

$$\sigma^2 \triangleq \text{var}\left(1-\lambda-\lambda\sum_{i=0}^{N-1} a_i W_i + \frac{1}{N}\sum_{i=0}^{N-1}(N_i - N_i')\right) = \left(\lambda\sigma_W\sqrt{\sum_i |a_i|^2}\right)^2 + \frac{\sigma_0^2+\sigma_1^2}{N}, \tag{44}$$

Interestingly, note that Problem 1 is equivalent to minimizing $\int_0^1 \dot{q}_I(t)^2 dt$ under Ass. 2. If this assumption is relaxed and smooth flow patterns are considered, one needs to solve the following straightforward calculus of variations problem.

Problem 2. *Minimizing $\int_0^1 \dot{q}_I(t)^2 dt$ under constraints:*

$$q_I(0) = q_I(1) = q_n, \quad \int_0^1 (q_I(t) - q_n)dt = 1. \tag{45}$$

Solution 2. *Problem 2 has a unique solution given by:*

$$q_I(t) = q^*(t) \triangleq q_n + 6t(1-t). \tag{46}$$

The value of the minimum is:

$$\int_0^1 (\dot{q}^*(t))^2 dt = 12. \tag{47}$$

Proof 2. *Note $Q(t) = \int_0^t (q_I(\tau) - q_n)d\tau$. Problem 2 is equivalent to the auxiliary problem of finding Q minimizing*

$$J(Q) \triangleq \int_0^1 \ddot{Q}^2(t)dt, \tag{48}$$

under the constraints:

$$Q(0) = 0, \quad Q(1) = 1, \quad \dot{Q}(0) = 0, \quad \dot{Q}(1) = 0. \tag{49}$$

The corresponding Euler-Lagrange equation is [5]:

$$\frac{d^2}{dt^2}\frac{d}{d\ddot{Q}}\ddot{Q}^2 = 0 \Leftrightarrow \frac{d^4}{dt^4}Q = 0. \tag{50}$$

Hence, Q is of the form $Q(t) = c_3t^3 + c_2t^2 + c_1t + c_0$. The constraints give a unique solution: $Q^*(t) = 2t^3 - 3t^2$. As J is convex, Q^* is the unique solution to the auxiliary problem. Hence, Problem 2 also has a unique solution given by:

$$\begin{aligned} q^*(t) &= q_n + \dot{Q}^*(t) \\ &= q_n + 6t(1-t). \end{aligned} \tag{51}$$

The calculation of the corresponding value $\int_0^1 (\dot{q}^*(t))^2 dt$ is straightforward.

5. Simulation Results

We now study the performance of the loss detection algorithm on a theft scenario simulation for various input patterns. In Fig. 4, we represent a conveyor belt connecting a production site to a storage facility. The flow of bulk material is steady with nominal value q_n except for punctual overloads (of unitary time, without loss of generality) randomly appearing with probability p_1. In such a case, the shape of the overloads is controlled by a flow input pattern q_I. Somewhere along the conveyor, a group of thieves may steal bulk material. One would like to detect this robbery.

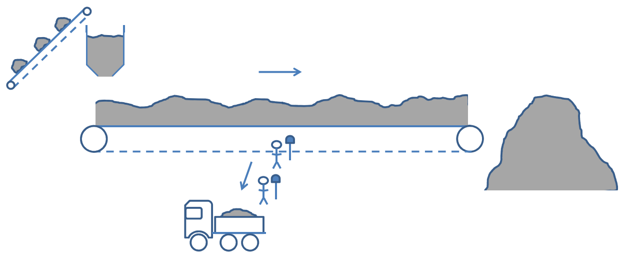

Fig. 4: Theft scenario.

We simulate N_{simu} unitary windows. On every window, we consider two theft scenarios:

- Basic theft: the thieves act randomly (for example whenever they are free of surveillance) with probability p. When they do so, they reroute a fraction $1-\lambda$ of the flow (steady or overload), λ following the *pdf* f^Λ.
- Smart theft: the thieves act with the same *modus operandi* but only on the overloaded windows.

We use the following parameters: $N = 20$, $\delta = 0.08$, $\alpha = 0.6$, $\beta = 0.9$, $p = 0.3$, $\sigma_0 = \sigma_1 = 0.1$, $b^* = 0.09$, $N_{simu} = 100000$, $p_1 = 0.2$.

We compare the performance of the loss detection algorithm on those two cases for four different overload controlled input pattern represented in Fig. 5. The considered flows are the optimal patterns computed in Section 4. , as well as a reference piecewise affine pattern q^a and a reference smooth pattern q^s. As expected, we observe a strong similarity between both optimal patterns, $q^\# \simeq q^*$. It is easy to show that $q^\#$ converges uniformly to q^* as N goes to infinity.

The rate of loss detection and of false alarms for the four flow patterns and the two theft strategies are gathered in Tab. 2. The smart theft strategy is clearly more efficient from the thief's viewpoint. For all the input patterns the losses are less detected, and the rate of false alarms is much higher, which, in turn, deteriorates the reliability of the theft surveillance. Also, the

Tab. 2: Impact of the input flow pattern and the theft strategy on the algorithm performance.

time uncertainty: $\delta = 0.08$	**random theft**		**smart theft**	
	detections	false alarms	detections	false alarms
q^a (ref.)	96.8 %	3.1 %	95.3 %	11.0 %
$q^\#$ (opt.)	97.0 %	1.5 %	95.9 %	5.9 %
q^s (ref.)	96.8 %	2.2 %	95.7 %	8.4 %
q^* (opt.)	97.2 %	1.6 %	96.6 %	5.8 %
no time uncertainty: $\delta = 0$				
q^a (ref.)	97.3 %	0.5 %	97.3 %	2.2 %
$q^\#$ (opt.)	97.2 %	0.6 %	97.6 %	2.5 %
q^s (ref.)	97.1 %	0.5 %	97.4 %	2.4 %
q^* (opt.)	97.2 %	0.5 %	97.4 %	2.2 %

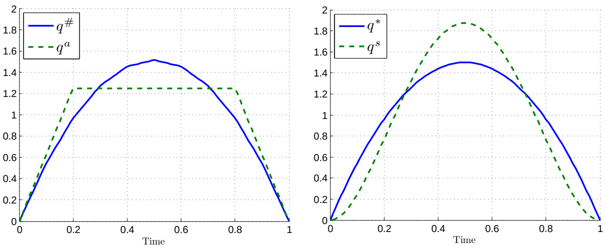

Fig. 5: Optimal and reference flow input patterns, piecewise affine (left) and smooth (right).

optimal patterns yield better overall performance than the reference ones, especially regarding false alarms. This difference is however smaller than the impact of theft strategy. The false alarms are partly due to measurement noise and partly to time uncertainty δ. To emphasize the contribution of time uncertainty on the algorithm performance, the same simulation has been run with $\delta = 0$.

6. Conclusions and Perspectives

The study conducted in this article has shown that the problem of accurate data timing, which surprisingly has not generated significant theoretical studies before, is of true importance for online monitoring applications. The analysis has been performed on a very simple model, allowing one to derive explicit formulas for estimator variance and probabilities of detection and false alarms. Solutions to mitigate this malicious effect have been derived. For the "naive" average imbalance estimator, the variance is scaled by the L^2 norm of the input flow. More generally, investigations shall be focused on determining to which extent this conclusion holds for more advanced estimation methods such as (extended) Kalman filtering or state observers, in various contexts. Also, applying the same methodology to more complex flow dynamics such as water hammer equation for liquid pipelines is a topic for future research.

References

[1] API 1130 *Computational Pipeline Monitoring for Liquids Pipelines*. Washington: American Petroleum Institute, 2002.

[2] BARS, R., P. COLANERI, L. DUGARD, F. ALLGOWER, A. KLEIMENOV and C. SCHERER. Trends in theory of control system design. In: *Proc. 17th Internetional Federation of Automatic Control World Congress*. Seoul: IFAC, 2008, pp. 2144–2155. ISBN 978-3-902661-00-5. DOI: 10.3182/20080706-5-KR-1001.00363.

[3] BEGOVICH, O., A. NAVARRO, E. N. SANCHEZ and G. Besancon. Comparison of two detection algorithms for pipeline leaks. In: *CCA - 16th IEEE International Conference on Control Applications*. Singapore: IEEE, 2007, pp. 777–782. ISBN 978-1-4244-0442-1. DOI: 10.1109/CCA.2007.4389327.

[4] BOYD, S. and L. VANDENBERGHE. *Convex Optimization*. Cambridge: Cambridge University Press, 2004. ISBN 0-521-83378-7.

[5] BRYSON, A. E. and Y. HO. *Applied Optimal Control: optimization, estimation, and control*. Carlsbad: Hemisphere Publishing Company, 1975. ISBN 0-89116-228-3.

[6] DUDEK, M. Liquid Leak Detection Focused on Theft Protection. In: *OnePetro* [online]. 2005. Available at: `https://www.onepetro.org/conference-paper/PSIG-05A4`.

[7] ENSMINGER, D. and L. J. BOND. *Ultrasonics fundamentals, technologies, and applications*. Boca Raton: CRC Press, 2011. ISBN 978-0-8247-5889-9.

[8] FALCIMAIGNE, J. and S. DECARRE. *Multiphase production: Pipeline Transport, Pumping and Metering*. Paris: Editions OPHRYS, 2008. ISBN 978-2-7108-0913-5.

[9] FRADEN J. *Handbook of modern sensors: physics, designs and applications*. New York:

Springer, 2010. ISBN 978-1-4419-6465-6. DOI: 10.1007/978-1-4419-6466-3.

[10] FRERIS, N. M., V. S. BORKAR and P. R. KUMAR. A mode-based approach to clock synchronization. In: *48th IEEE Conference on Decsion and Control*. Shanghai: IEEE, 2009, pp. 5744–5749. ISBN 978-1-4244-3871-6. DOI: 10.1109/CDC.2009.5399516.

[11] FRERIS, N. M., S. R. GRAHAM and P. R. KUMAR. Fundamental Limits on Synchronizing Clocks Over Networks. *IEEE Transactions on Automatic Control*. 2011, vol. 56, iss. 6, pp. 1352–1364. ISSN 0018-9286. DOI: 10.1109/TAC.2010.2089210.

[12] GEIGER, G. State-of-the-Art in Leak Detection and Localisation. *Oil Gas European Magazine*. 2006, vol. 32, iss. 4, pp. 193–198. ISSN 0342-5622.

[13] HOKAYEM, P. F. and M. W. SPONG. Bilateral teleoperation: An historical survey. *Automatica*. 2006, vol. 119, iss. 12, pp. 2035–2057. ISSN 0005-1098. DOI: 10.1016/j.automatica.2006.06.027.

[14] MONTGOMERY, D. C. and G. C. RUNGER. *Applied Statistics and Probability for Engineers*. Jefferson City: Wiley, 2010. ISBN 978-0470053041.

[15] MURRAY, R., K. ASTROM, S. BOYD, R. BROCKETT and G. STEIN. Future directions in control in an information-rich world. *Control Systems*. 2003, vol. 23, iss. 2, pp. 20–33. ISSN 1066-033X. DOI: 10.1109/MCS.2003.1188769.

[16] PERRY, R. H. and D. W. GREEN. *Perry's Chemical engineers handbook*. New York: McGraw-Hill, 2007. ISBN 978-0702040429.

[17] RAHIMAN, W., B. LI, B. WU and Z. DING. Circle Criterion Based Nonlinear Observer Design For Leak Detection In Pipelines. In: *ICCA - International Conference on Control and Automation*. Guangzhou: IEEE, 2007, pp. 2993–2998. ISBN 978-1-4244-0818-4. DOI: 10.1109/ICCA.2007.4376911.

[18] SONBUL, O., P. POPEJOY and A. N. KALASHNIKOV. Ultrasonic Sensor array for remote sensing of profiles of bulk materials. In: *I2MTC - International Instrumentation and Measurement Technology Conference*. Graz: IEEE, 2012, pp. 1794–1797. ISSN 1091-5281. DOI: 10.1109/I2MTC.2012.6229189.

[19] ZEZULKA, F., Z. BRADAC, P. FIEDLER and M. SIR. Trends in Automation - investigation in Newtork Control Systems and Sensor Networks. In: *10th IFAC Workshop on programmable devices and embedded system*. Gliwice: International Federation of Automatic Control, 2010, pp. 109–113. ISBN 978-3-902661-95-1. DOI: 10.3182/20101006-2-PL-4019.00022.

About Authors

Lionel MAGNIS is Ph.D. candidate in Mathematics and Control at MINES ParisTech. He was born in 1985 in Saint-Mande, France. He obtained his Master's Degree from MINES ParisTech in 2008. His research interests includes the theory of automatic control, signal processing and observer design.

Nicolas PETIT is Professor at MINES ParisTech and head of Centre Automatique et Systemes. He was born in 1972 in Paris, France. He graduated from Ecole Polytechnique in 1995 (X92), and obtained his Ph.D. in Mathematics and Control at MINES ParisTech in 2000 and his Habilitation a Diriger des Recherches from Universite Paris 6 in 2007. His research interests includes the theory of automatic control, distributed parameter systems, constrained trajectory generation, delay systems and observer design. On the application side, he is active in industrial process control. He has developed the controllers of several industrial chemical reactors, and the patented softwares ANAMEL 4 and 5, currently in use for closed-loop control of blending devices in numerous refineries at the TOTAL company.